



## Communication—Poly(ethylene oxide)-Immobilized Ionogel with High Ionic Liquid Loading and Superior Ionic Conductivity

Shufeng Song,<sup>a,z</sup> Shan Yang,<sup>b</sup> Feng Zheng,<sup>b</sup> Kaiyang Zeng,<sup>b</sup> Hai Minh Duong,<sup>b</sup> Serguei V. Savilov,<sup>c</sup> Serguei M. Aldoshin,<sup>c</sup> Ning Hu,<sup>a,d</sup> and Li Lu<sup>b,e,z</sup>

<sup>a</sup>College of Aerospace Engineering, Chongqing University, Chongqing 400044, People's Republic of China

<sup>b</sup>Materials Science Group, Department of Mechanical Engineering, National University of Singapore, Singapore 117575

<sup>c</sup>Department of Physical Chemistry Engineering, M.V. Lomonosov Moscow State University, Moscow, Russia

<sup>d</sup>The State Key Laboratory of Mechanical Transmissions, Chongqing University, Chongqing 400044, People's Republic of China

<sup>e</sup>National University of Singapore Suzhou Research Institute, Suzhou, People's Republic of China

Immiscibility between polymer and ionic liquid, and the loss of solid-state configuration when ionic liquid loading becomes too high have been addressed by creating poly(ethylene oxide)-immobilized ionogel through a facile mechanochemical method. The poly(ethylene oxide)-immobilized ionogel with ionic liquid loading as high as 50 wt% demonstrates a high room-temperature ionic conductivity in the order of  $10^{-4}$  S cm<sup>-1</sup>.

© 2016 The Electrochemical Society. [DOI: 10.1149/2.0311614jes] All rights reserved.

Manuscript submitted August 25, 2016; revised manuscript received October 12, 2016. Published October 25, 2016.

Liquid state limits the potential application of ionic liquids (ILs) due to ineffectiveness in mitigating lithium dendrite growth in lithium-based batteries.<sup>1</sup> Numerous efforts have been devoted to immobilize ILs in solid-state matrices, also known as ionogels.<sup>2</sup> If ILs are immobilized in polymer matrices to form freestanding membranes to integrate high conductivities of ILs, solid flexibility of polymers can be easily used to make solid-state batteries.<sup>3,4</sup> However, the development of polymer-supported ionogels has been hampered by two issues, one of which is the immiscibility between polymers and ILs, and another is the loss of solid-state configuration of the polymers when high loading ILs are used.<sup>2</sup>

We propose here a simple strategy to overcome the immiscibility between polymer and IL and the loss of solid-state configuration when IL loadings are too high, and to create polymer-immobilized ionogel characterizing high IL loading and superior ionic conductivity.

### Experimental

A mixture of poly(ethylene oxide) (PEO, 100 000 g mol<sup>-1</sup>), LiClO<sub>4</sub> ([EO]:[Li] = 10:1), SiO<sub>2</sub> (10 wt%, 5–15 nm) and 1-butyl-1-methylpyrrolidinium bis(trifluoromethylsulfonyl)imide (BMPTFSI) was stirring 2 h in acetone, followed by high energy ball milling (SPEX SamplePrep 8000M) for 1 h and subsequently was casted on PTFE plate and dried at 50°C in vacuum.

The ionic conductivity was measured from 1 MHz to 1 Hz (Solartron, 1260+1287) in a cell sandwiching the ionogel (0.42 mm in thickness and 10 mm in diameter) between stainless steels. The Arrhenius plot for the ionogel was obtained at the temperature range of 27°C and 110°C. The variation of the conductivities was monitored with time via impedance of same sample. The ionogel was examined by X-ray diffraction (Shimadzu XRD-7000), SEM (S-4300 Shimadzu), Atomic Force Microscopy (AFM, MFP-3D, Asylum Research) as well as XPS (Axis Ultra DLD, Shimadzu).

### Results and Discussion

A stable resin is obtained after the processing of mechanochemical activation (Figure 1a). A freestanding, transparent and flexible ionogel membrane is obtained after the resin solidifies (Figure 1b). Different from formic acid-activated sol-gel processes which usually needed several days to gelate and solidify,<sup>5</sup> such synthetic strategy is ultra-effective, and the most important key is to overcome the immiscibility between polymers and ILs, and to achieve IL loading as

high as 50 wt%. With the help of this synthesis strategy, different PEO-immobilized ionogels with high IL loadings can be created by employing various ILs. Here, we focus on the 50 wt% of BMPTFSI ionogel owing to its outstanding conductivity and practically useful mechanical performance (i.e. freestanding membrane), as compared to 20 wt% by the mainstream solution-based methods reported previously.<sup>6,7</sup> The 'free-standing' means that the membrane can be handled, but no traditionally mechanical strength. The addition of ionic liquid would improve the ionic conductivities of PEO-based polymers, on the other hand, would plasticize the PEO chains and make the membranes sticky. In the present work, it is hard to handle the membranes when amount of BMPTFSI is above 50 wt%. The PEO-immobilized BMPTFSI ionogel reveals a well-defined and disordered dendritic morphology as shown in Figure 1c, which is different from the spherulitic morphologies of typical PEO-LiX polymers.<sup>8</sup> The surface of such ionogel is smooth, as compared to the rough surfaces of pure PEO-LiX polymers,<sup>9</sup> indicating an amorphous structure. As shown in the AFM image, the bright areas of the ionogel represent the distribution of silicon-based matrix (Figure 1d), since the bright zones represent higher energy dissipation, while the dark zones are attributed to domains of PEO and BMPTFSI owing to more inelasticity.

The initial room-temperature conductivity of polymer electrolyte without IL is calculated to be  $1.25 \times 10^{-5}$  S cm<sup>-1</sup> based on the interception of semicircle (Figure 2a), which is comparative to the reported values.<sup>10–12</sup> Unlike the polymer electrolytes, the semicircle of the impedance of the ionogel at high frequency range disappears with only a capacitive tail (Figure 2a), which is similar to the case for many gel polymer electrolytes.<sup>13</sup> A possible reason may be that the cations have a weak dielectric relaxation owing to the fast cations transport in IL-containing ionogels, thus resulting in a weak capacitive effect of the ionogels in the impedance spectrum. The intercept of the spike on the real axis is assigned to the bulk resistance for the ionogel. The initial room-temperature conductivity of the ionogel is calculated to be  $7.28 \times 10^{-4}$  S cm<sup>-1</sup> (Figure 2a), which is well above the practically useful value of  $10^{-4}$  S cm<sup>-1</sup> required for application in energy storage batteries.<sup>14</sup> Such conductivity is at least three orders of magnitude higher than those of PEO-LiX polymer electrolytes and one order of magnitude higher than those of the PEO-LiX-SiO<sub>2</sub> polymer electrolytes,<sup>10–12,15</sup> though lower than that of the pristine BMPTFSI ( $\sim 2.4$  mS cm<sup>-1</sup>) but closer.<sup>16</sup> Figure 2b displays the variation of room-temperature ionic conductivities of ionogel and polymer electrolyte without IL with time. For the polymer electrolyte without IL, the conductivity decays fast with time (i.e. from  $10^{-5}$  S cm<sup>-1</sup> to  $10^{-6}$  S cm<sup>-1</sup> after one week). For the ionogel, the conductivity has some decays to ca.  $1.5 \times 10^{-4}$  S cm<sup>-1</sup> after 6 days, afterwards

<sup>z</sup>E-mail: sfsong@cqu.edu.cn; luli@nus.edu.sg

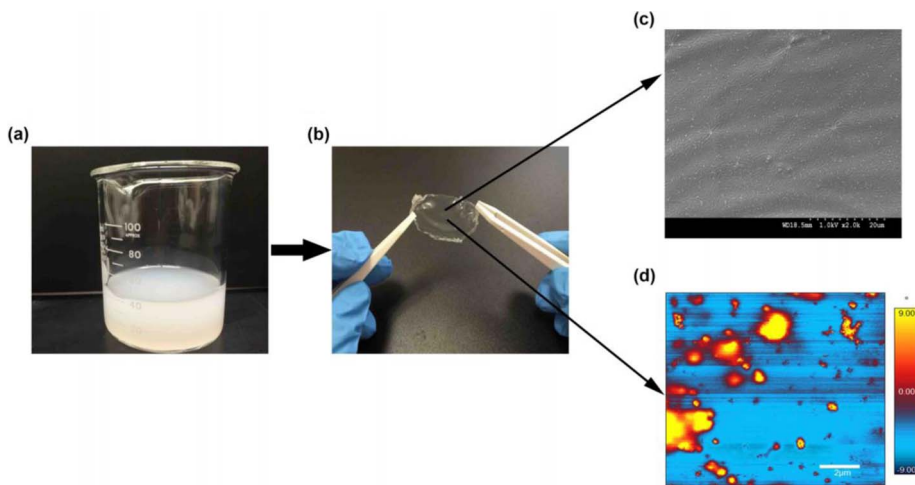


**Figure 1.** The PEO-immobilized ionogel: (a) A resin obtained from high energy ball milling. (b) Typical obtained ionogel membrane after solidifying. (c) SEM image of the ionogel membrane. (d) AFM phase image of the ionogel membrane.

is quite stable. The recrystallization of PEO at room temperature leads to the quick decrease of conductivity within one week. Maranas et al. reported that PEO-based polymer electrolytes underwent recrystallization below  $60^{\circ}\text{C}$ , which decreased the conductivities by more than two orders of magnitude at room temperature.<sup>17</sup> The conductivity of ionogel is stable at  $\sim 1.5 \times 10^{-4} \text{ S cm}^{-1}$  after 6 days, indicating the recrystallization of PEO is partially inhibited. XRD results show that the as-prepared ionogel is fully amorphous at room temperature, but partially crystalline after stored 15 days in Ar-filled glove box (Figure 2c). The recrystallization of PEO-based polymer electrolytes below  $\sim 60^{\circ}\text{C}$  and with time is a main issue which prevents their use in more applications, through which the conductivities are severely decreased. It is accordingly deduced that the ionogel presents a unique feature of superior conduction performance. A reasonable interpretation of this behavior is probably that, a combination of the plasticization of PEO

induced by BMPTFSI and the interaction of PEO and BMPTFSI during high energy ball milling, depresses the recrystallization of PEO networks as a result of nearly amorphous state at room temperature. The activation energy of ionogel is calculated to be 0.4 eV from the Arrhenius plot (Figure 2d).

It is worth to mention that the XPS spectra obtained are different from those known for individual substances (Figure 3). The peak area ratio for components 286.3 eV and 284.8 eV in C1s spectrum for the ionogel is more than one, while for PEO<sub>10</sub>-LiClO<sub>4</sub> system should be below.<sup>18</sup> The N1s spectrum of 399.2 and 402.3 eV corresponds to the nitrogen atoms of the anion and cation, respectively.<sup>19</sup> However, the ratio between them is different from expected value for BMP TFSI (1:1). The binding energy of silicon atoms (102.0 eV) is less than known for SiO<sub>2</sub> (103.0–103.6 eV), indicating possible formation of siloxanes.<sup>20,21</sup> Spectrum of sulfur atoms also differs from the known

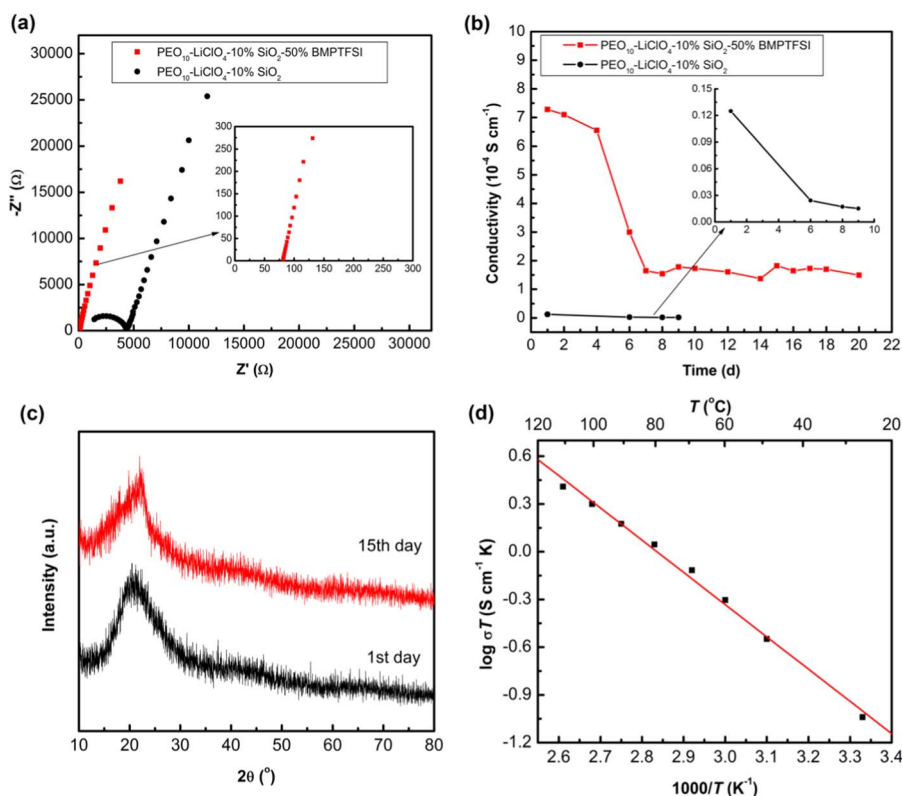


**Figure 2.** (a) The impedance plots of the as-prepared ionogel and polymer electrolyte without ionic liquid at room temperature. (b) The time evolution of room-temperature conductivities of the ionogel and polymer electrolyte without ionic liquid. (c) XRD patterns of the ionogel as prepared for 1 day and 15 days. (d) Arrhenius plot for the ionogel.

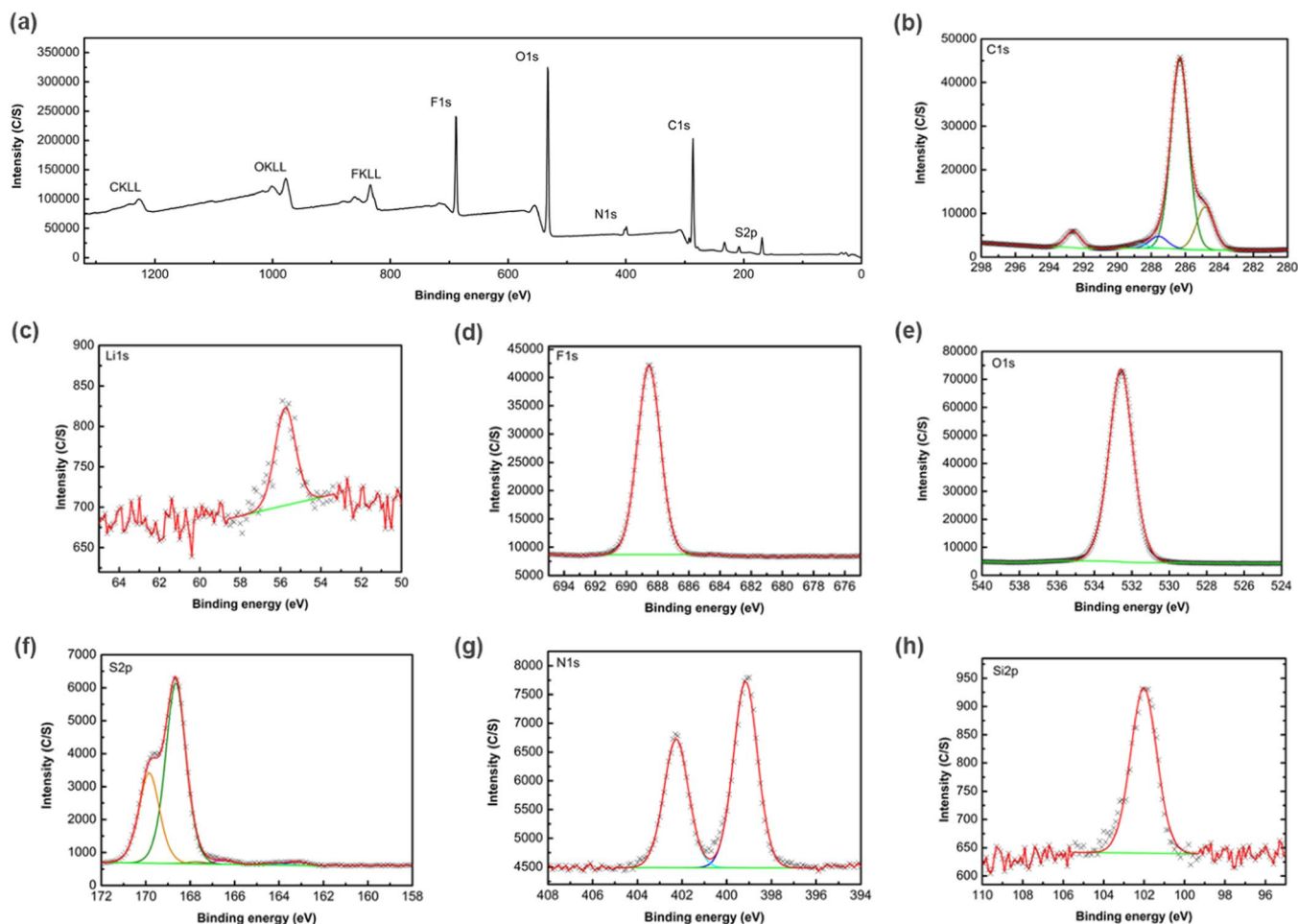


**Figure 3.** XPS spectra of the PEO-immobilized ionogel: (a) XPS spectra, (b) C1s spectrum, (c) Li1s spectrum, (d) F1s spectrum, (e) O1s spectrum, (f) S2p spectrum, (g) N1s spectrum, (h) Si2p spectrum.

for TFSI<sup>-</sup> due to presence of low intensive components at 163.2 and 166.5 eV, corresponding to reduced sulfur forms.<sup>20</sup> All these facts demonstrate the red-ox processes in ionogel at least for IL and SiO<sub>2</sub> and point out the interactions between PEO and silica. Thus, the data obtained demonstrate the integrated structure of ionogel.

### Summary

New ionogel with PEO scaffold and BMPTFSI percolating phase is developed by facile mechanochemical method to overcome the immiscibility between polymer and IL, and the limitation of IL loadings. The ionogel characterizes a true solid-state, freestanding, transparent and flexible membrane, moreover a practically useful and stable room-temperature ionic conductivity. The present work might inspire people to understand how “mechanochemistry” solving the immiscibility and inducing the interaction between polymers and ILs thereby might open up opportunity for designing new polymer electrolytes.

### Acknowledgments

This work is supported by Chongqing University, the Fundamental Research Funds for the Central Universities (No. 0241005202014, No. 0903005203403), National Natural Science Foundation of China (No. 51572182, No. 11372104, No. 11372363, No. 11332013, No. 5121543 and No. 11632004), National University of Singapore, the National Research Foundation, Prime Minister’s Office, Singapore under its Competitive Research Programme (CRP Award No. NRF-CRP 8-2011-04), as well as Russian Science Foundation (Project 14-43-00072).

### References

1. K. J. Harry, X. Liao, D. Y. Parkinson, A. M. Minor, and N. P. Balsara, *J. Electrochem. Soc.*, **162**, A2699 (2015).
2. J. Le Bideau, L. Viau, and A. Vioux, *Chem. Soc. Rev.*, **40**, 907 (2011).
3. A. S. Fisher, M. B. Khalid, and P. Kofinas, *J. Electrochem. Soc.*, **159**, A2124 (2012).
4. J. Shin, W. A. Henderson, and S. Passerini, *J. Electrochem. Soc.*, **152**, A978 (2005).
5. M. Neouze, J. Bideau, F. Leroux, and A. Vioux, *Chem. Commun.*, **8**, 1082 (2005).
6. D. D. Girolamo, S. Panero, M. A. Navarra, and J. Hassoun, *J. Electrochem. Soc.*, **163**, A1175 (2016).
7. S. K. Chaurasia, R. K. Singh, and S. Chandra, *J. Polym. Sci., Part B: Polym. Phys.*, **49**, 291 (2011).
8. J. M. Marentette and G. R. Brown, *J. Chem. Educ.*, **70**(6), 435 (1993).
9. E. M. Fahmi, A. Ahmad, M. Y. A. Rahman, and H. Hamzah, *J. Solid State Electrochem.*, **16**, 2487 (2012).
10. F. Croce, G. B. Appetecchi, L. Persi, and B. Scrosati, *Nature*, **394**, 456 (1998).
11. T. Chatterjee, K. Yurekli, V. G. Hadjiev, and R. Krishnamoorti, *Adv. Funct. Mater.*, **15**, 1832 (2005).
12. L. Y. Yang, D. X. Wei, M. Xu, Y. F. Yao, and Q. Chen, *Angew. Chem. Int. Ed.*, **53**, 3631 (2014).
13. H. C. Gao, B. K. Guo, J. Song, K. Park, and J. B. Goodenough, *Adv. Energy Mater.*, **5**, 1402235 (2015).
14. M. W. Schulze, L. D. McIntosh, M. A. Hillmyer, and T. P. Lodge, *Nano Lett.*, **14**, 122 (2014).
15. F. Croce, R. Curini, A. Martinelli, L. Persi, F. Ronci, and B. Scrosati, *J. Phys. Chem. B*, **103**, 10632 (1999).
16. M. K. Singh, Y. Kumar, and S. A. Hashmi, *Nanotechnology*, **24**, 465704 (2013).
17. S. K. Fullerton-Shirey and J. K. Maranas, *Macromolecules*, **42**, 2142 (2009).
18. D. Martin-Vosshage and B. V. R. Chowdari, *J. Electrochem. Soc.*, **142**, 1442 (1995).
19. F. Buchner, M. Bozorgchenani, B. Uhl, H. Farkhondeh, J. Bansmann, and R. Jürgen Behm, *J. Phys. Chem. C*, **119**, 16649 (2015).
20. M. C. Capel-Sanchez, L. Barrio, J. M. Campos-Martin, and J. L. G. Fierro, *J. Colloid Interf. Sci.*, **277**, 146 (2004).
21. A. Watanabe, M. Fujitsuka, and O. Ito, *Thin Solid Films*, **354**, 13 (1999).